Reprinted from October 1986, Vol. 108, Journal of Engineering Materials and Technology

Macro-Mechanical Analysis for Symmetric and Asymmetric Fully Plastic Crack Growth

G. A. Kardomateas[1]

Massachusetts Institute of Technology, Cambridge, MA 02139

Asymmetries like welds or shoulders, may eliminate one of the two shear zones of symmetrically fully plastic cracked parts and thus give crack propagation along the remaining active slip band through pre-strained material instead of through the relatively unstrained region between two shear bands of the symmetric case. One thus expects a reduced ductility in the single shear band asymmetric case. A macro-mechanical analysis provides a physical basis for explaining the development of deformation in both geometries, as observed from tests on several alloys. The asymmetric case is approximated as Mode II shearing, with the crack extension occurring by sliding off along a single slip plane and fracture. In the symmetric Mode I case, the crack is assumed to extend by alternating shear on two symmetric slip planes and fracture.

Introduction

In studying fracture there is a need for understanding the development of deformation in the fully plastic range for both the usual symmetric and the asymmetric case depicted in Fig. 1. The asymmetric configuration may occur practically near welds due to the constraint of the heat affected zone or due to some geometric asymmetry, for example near shoulders. These cracks exhibit less ductility than symmetric ones [1], because the crack is advancing into prestrained and damaged material rather than the new material encountered by a crack advancing between two symmetrical shear bands. Near the tip of the growing crack, strain hardening will cause the deformation field to fan out. For power law creep or deformation theory plasticity, the stress and strain in the neighborhood of a stationary crack may be found from Shih's [2] mixed mode solutions which can be integrated quasi-steadily [3]. More realistically, a corresponding, fully-plastic, incremental plasticity solution should be obtained for a growing crack, taking into account the hardening of the material left behind the growing crack. However the stress and strain at the crack tip may arise, they cause damage [4], for instance by hole nucleation and growth from inclusions. A macro-mechanical model would allow understanding the underlying physical mechanisms that lead to the different ductility in the two geometries. In the asymmetric case, assume that the crack jumps to the damaged site, and that sliding off along a single slip plane occurs by the amount of the crack tip displacement required to cause further cracking. The combination of cracking and sliding off gives the two new surfaces of the macro fracture. These define the crack opening angle and the crack direction. The process is then repeated. In the symmetric case the crack advances by alternating shear along the two symmetric slip planes as well as fracture. Notice that in a more general case there may be two slip planes at arbitrary angles. These ideas will now be developed quantitatively, giving a representation of crack growth from a single band or from the usual symmetric case with two slip bands.

Macro-Analysis

The Asymmetric Case. Consider a single shear band at an angle θ_s from the transverse. Although for an isotropic material slip occurs at 45 deg, a general angle θ_s will be used in considering the development of the deformation. Assume that

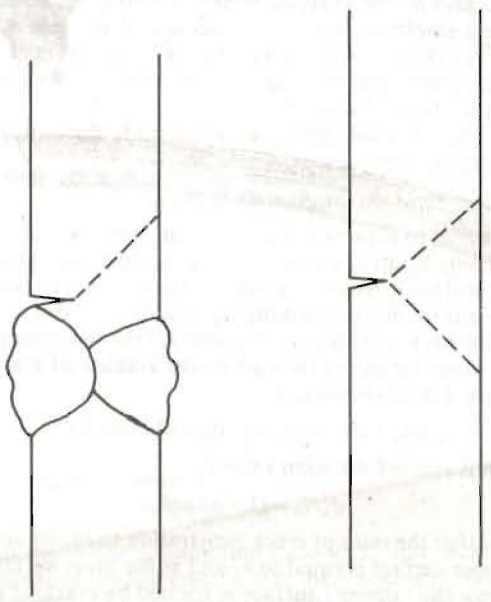

Fig. 1 Asymmetric and symmetric shear from a crack

[1]Present address: General Motors Research Laboratories, Engineering Mechanics Department, RMB-256, Warren, MI 48090-9055.

Contributed by the Materials Division for publication in the JOURNAL OF ENGINEERING MATERIALS AND TECHNOLOGY. Manuscript received by the Materials Division, November 25, 1985.

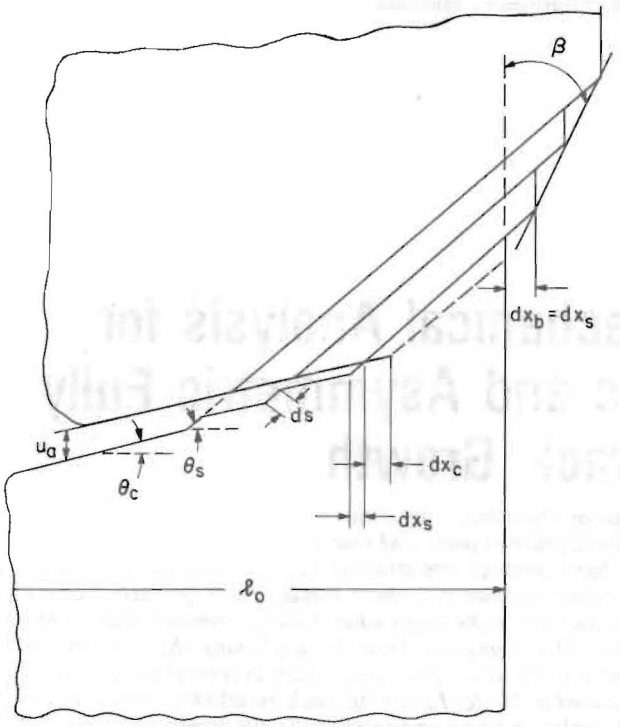

Fig. 2 Development of deformation for the asymmetric case

the fracture strain is large compared to the yield strain, so that fully plastic conditions prevail. Cracking to the new site occurs at an angle θ_c, smaller than θ_s, followed by sliding off. When the process is repeated as shown in Fig. 2, the upper surface consists entirely of "cracked" material, whereas the lower surface consists of a mixture of sheared-off and cracked material. The crack is thus assumed to grow by an amount dx_c due to cracking and then by an amount dx_s due to slipping along the plane making an angle θ_s with the normal to the load; these quantities are the projected values on the transverse direction. At the same time the back surface opposite the groove will be drawn in by an amount $dx_b = dx_s$. In the following analysis the independent variables will be taken to be the cracking orientation, θ_c, and the ratio of the projected lengths of the upper and lower flanks, $\lambda = l_u/l_l$. This is also the ratio of projected cracking to total reduction of the ligament thickness in the upper flank, $x_c/(x_c + x_s)$. The first dependent variable of interest is the ratio of the final axial deformation, u_a, to the initial ligament thickness, l_0. Two angles are of interest: θ_u and θ_l, the angles between the faces of the crack and the normal to the load direction, and the angle that the deformed back surface makes to the load axis, β.

The ratio of axial extension increment to ligament thickness u_a/l_0 can be expressed as

$$du_a/l_0 = dx_s \tan\theta_s/l_0. \tag{1}$$

It is desired to express this quantity in terms of θ_s and the projected length ratio, $\lambda = dx_c/dl$. The ligament thickness at the upper surface is reduced to zero by the distance of penetration of the groove due to cracking, x_c, and by that due to drawing in of the back surface, $x_b = x_s$, whereas the ligament thickness at the lower surface is reduced by the amount of cracking, x_c, and that due to slipping, x_s,

$$dx_c + dx_s = dl, \text{ or, } dx_s/dl = (1 - \lambda), \tag{2}$$

and thus the deformation ratio is:

$$u_a/l_0 = (1 - \lambda)\tan\theta_s. \tag{3}$$

Notice that the ratio of crack penetration to initial ligament at the upper surface is equal to λ, and at the lower surface is unity. Since the "upper" surface is formed by cracking only, the "upper" angle is:

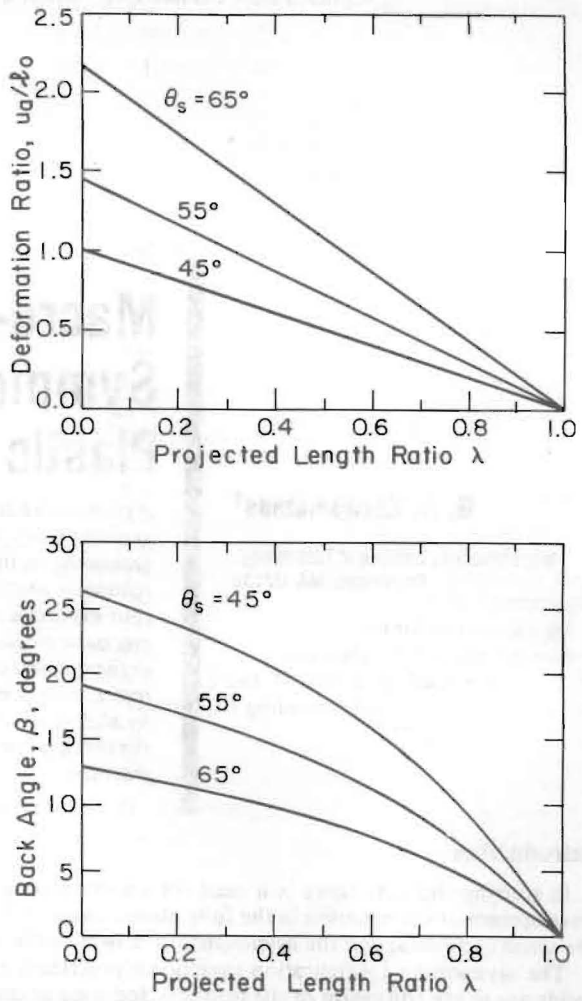

Fig. 3(a) Deformation ratio and back angle as functions of the slip angle θ_s and the projected length ratio λ for the asymmetric case

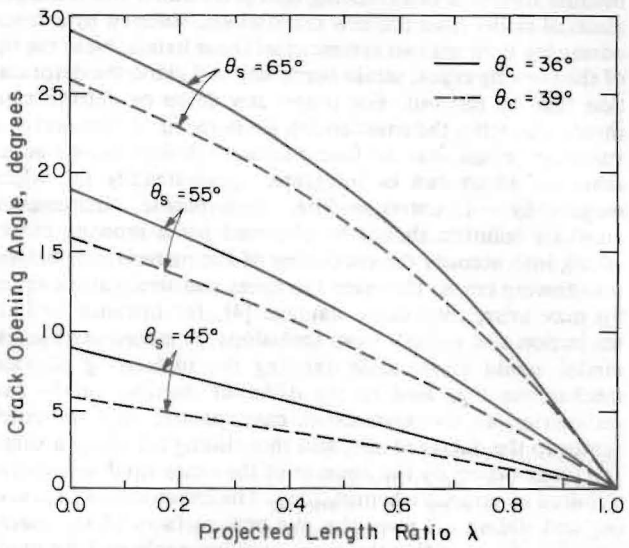

Fig. 3(b) Crack opening angle as a function of the projected length ratio λ for the asymmetric case

$$\theta_u = \theta_c. \tag{4}$$

The angle of the "lower" surface (for $\theta_c < \theta_s$) is found from Fig. 2:

$$\theta_l = \tan^{-1}\frac{dx_c\tan\theta_c + dx_s\tan\theta_s}{dx_c + dx_s}. \tag{5}$$

Substituting the above expressions for the cracking and slipping ratios dx_c/dl and dx_s/dl, gives the lower flank angle:

$$\theta_l = \tan^{-1}[(1-\lambda)\tan\theta_s + \lambda\tan\theta_c]. \tag{6}$$

The average fracture direction is then

$$\theta_f = (\theta_l + \theta_u)/2, \tag{7}$$

and the crack opening angle

$$\text{COA} = \theta_l - \theta_u. \tag{8}$$

The back angle β is found similarly from Fig. 2 and equation (2):

$$\beta = \tan^{-1}\frac{dx_b}{dl\tan\theta_s + dx_b\tan\theta_s} = \tan^{-1}\frac{1-\lambda}{(2-\lambda)\tan\theta_s}. \tag{9}$$

Fig. 3(*a*) shows the deformation ratio u_a/l_0 and the back angle β as functions of the slip angle θ_s and the projected length ratio λ. The displacement ratio and the back angle are larger for a smaller projected length ratio. In Fig. 3(*b*) the crack opening angle is plotted as a function of the projected length ratio λ and the slip angle θ_s for the cases of a cracking angle $\theta_c = 36$ deg and 39 deg. The higher value of θ_c was observed with the lower hardening alloys. The COA increases with decreasing λ and is larger for the smaller upper flank angle θ_c.

An expression for the shear strain may also be found. Referred to the axes of the slip, the deformation is pure shear and may be expressed in terms of the slip ds and the normal separation between corresponding slip planes:

$$\gamma = \frac{ds}{(dx_c/\cos\theta_c)\sin(\theta_s - \theta_c)}, \tag{10}$$

and with the aid of Fig. 2 and equation (2), this may be rearranged to give

$$\gamma = \frac{(1-\lambda)}{\lambda}\frac{\cos\theta_c}{\cos\theta_s\sin(\theta_s - \theta_c)}. \tag{11}$$

The Symmetric Case. To distinguish from the above asymmetric Mode II case, the slip angle for the symmetric Mode I case will be denoted by α. As shown in Fig. 4, the crack in both its upper and lower flanks is assumed to grow by an amount dx_c due to cracking and then by an amount dx_s due to slipping along the plane making an angle α with the normal to the load. At the same time, the back surface opposite the groove will be drawn in by an amount dx_b. The ratio of cracking to total reduction of the ligament thickness, $x_c/(x_c + x_s + x_b)$, will be denoted here by q. The dependent variables of interest are again the ratio of the final deformation, u_a, to the initial ligament, l_0, and the ratio of the penetration of the crack to the point of final separation divided by the initial ligament, P/l_0. Two angles can also be found: δ, the angle between crack flank and the transverse direction, and the angle that the deformed back surface makes to the load axis, β.

The ratio of axial extension increment to ligament thickness, du_a/l_0, can be expressed as

$$du_a/l_0 = 2dx_s\tan\alpha/l_0. \tag{12}$$

In order to express this quantity in terms of α and the "cracking ratio", q, we notice again that the ligament thickness is reduced to zero by the distance of penetration of the groove due to cracking, x_c, by that due to slipping, x_s, and by that due to drawing in of the back surface x_b. Assuming that there is equal slip from the two sides of the groove, first from the top and then from the bottom, it can be seen from Fig. 4 and the definition of the cracking ratio, q, that

$$dx_s/dl = [1 - (dx_c/da)]/2 = (1-q)/2. \tag{13}$$

From (12), the ratio u_a/l_0 is then

$$u_a/l_0 = (1-q)\tan\alpha. \tag{14}$$

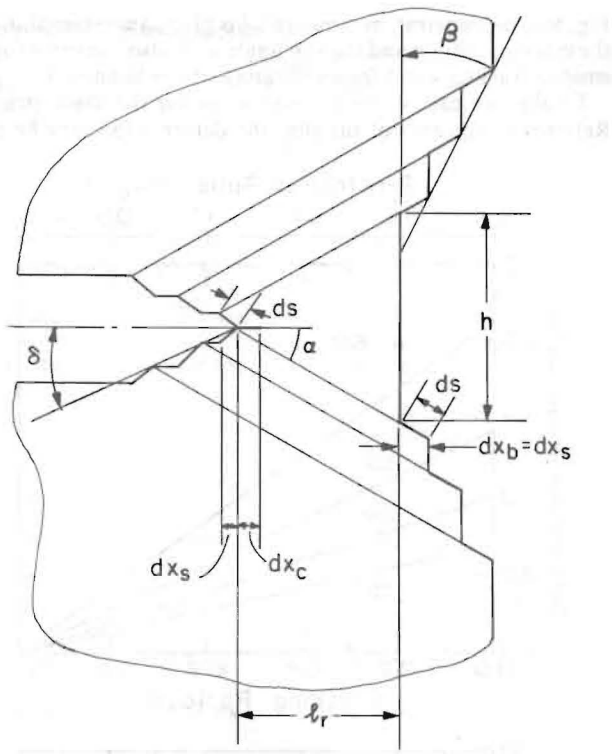

Fig. 4 Development of deformation for the symmetric case

We can also relate the deformation remaining to final separation, u_r, to the flat surface remaining at the back side of the specimen. Calling the height of this presently undeformed material, h, Fig. 4 indicates that h is given by

$$h = 2l_r\tan\alpha. \tag{15}$$

From (14) and (15), the ratio of the extension to flat height is:

$$u_r/h = (1-q)/2. \tag{16}$$

From the ratio dx_s/dl, as found in (13), the ratio of crack penetration to initial ligament thickness can be expressed in terms of the cracking ratio:

$$P/l_0 = \frac{dx_c + dx_s}{dx_c + 2dx_s} = (1+q)/2. \tag{17}$$

From Fig. 4 and the expressions for the cracking and slipping ratios, the penetration semiangle, δ, is found:

$$\delta = \tan^{-1}\frac{dx_s\tan\alpha}{dx_c + dx_s} = \tan^{-1}\frac{(dx_s/dl)\tan\alpha}{dP/dl}, \text{ or,}$$

$$\delta = \tan^{-1}\left(\frac{1-q}{1+q}\tan\alpha\right). \tag{18}$$

Notice that when there is no cracking, so that λ is equal to zero, the semiangle δ of the penetrating crack must be equal to the slip angle α.

In a similar fashion the back angle β can be found from Fig. 4 as:

$$\beta = \tan^{-1}\frac{dx_b}{(dx_c + 2dx_s)\tan\alpha + dx_b\tan\alpha}$$

$$= \tan^{-1}\frac{1-q}{(3-q)\tan\alpha}. \tag{19}$$

The crack opening angle is

$$\text{COA} = 2\delta. \tag{20}$$

Fig. 5(*a*) shows the deformation ratio u_a/l_0 and back angle β as functions of the slip angle α and the cracking ratio q. Both these quantities increase when the cracking ratio decreases. In

Fig. 5(*b*) the penetration semiangle δ is plotted as a function of the cracking ratio q and the slip angle α. It also increases for a smaller cracking ratio (more thinning of the ligament).

Finally, we can obtain an expression for the shear strain. Referred to the axes of the slip, the deformation may be expressed, as in the asymmetric case, in terms of the slip ds and the normal separation between corresponding slip planes:

$$\gamma = ds/[(ds)\sin 2\alpha + (dx_c)\sin\alpha].$$

With the aid of Fig. 4 and equation (13) this may be rearranged to give

$$\gamma = (1-q)/\sin 2\alpha. \tag{21}$$

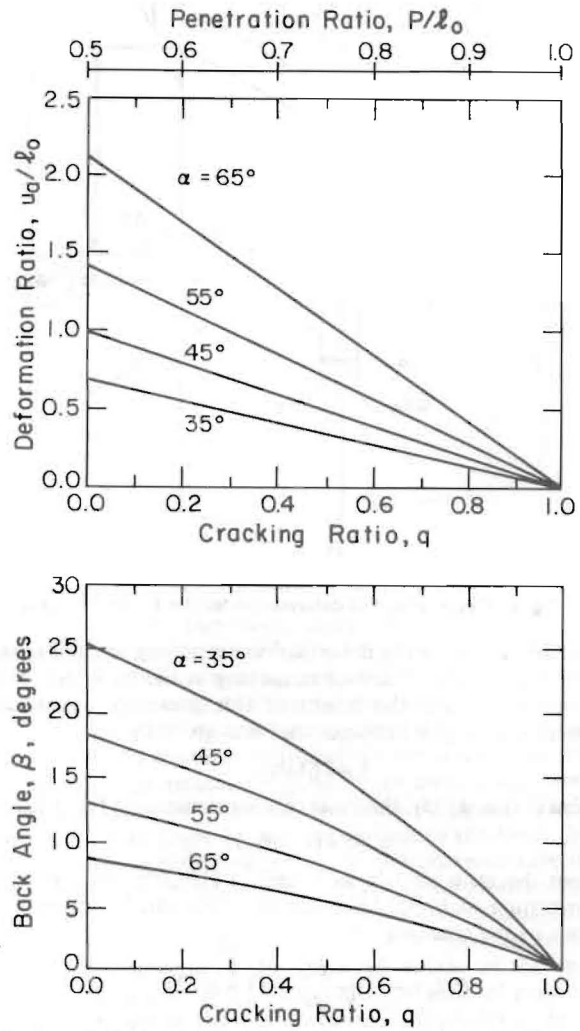

Fig. 5(*a*) Deformation ratio and back angle as functions of the slip angle α and the cracking ratio, q, for the symmetric case

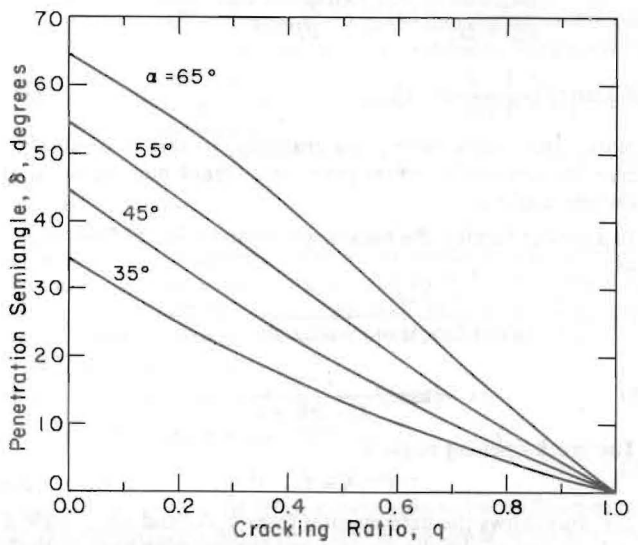

Fig. 5(*b*) Penetration semiangle as a function of the cracking ratio q (symmetric case)

Experimental Results

The experimental investigation included testing symmetric and asymmetric specimens for the lower hardening 1018 cold finished, HY-80 and HY-100 steel and the higher hardening A36 hot rolled, 1018 normalized steel [1]. In the asymmetric configuration (asymmetry introduced through a shoulder), the lower hardening alloys showed more than 3 times smaller displacement to fracture than the symmetric; the higher hardening alloys showed however only up to 20 percent reduction [1]. To obtain the flank lengths, the flank angles, the back angle and the displacement to separation, the profiles of the fracture surface and the deformed back surface were plotted with a travelling stage microscope.

To correlate with the above model in the asymmetric case, the projected crack length ratio λ (upper flank length per initial ligament l_0) was measured from the profiles of the fracture surface. This quantity, tabulated in Table 1, depends on the strain hardening and varies from 0.890 for the low hardening 1018 cold finished to 0.750 for the high hardening A36 hot rolled steel. The experimental data for λ and the upper flank angle θ_c were used in equations (1)–(9) for an assumed shear direction $\theta_s = 45$ deg to yield the displacement ratio, the lower flank angle θ_l and the back angle β. As an example, results for HY-80 and A36 hot rolled steels, compared with the experimental findings, are shown in Table 2. The crack opening angle, $\theta_l - \theta_u$, is bigger for the higher hardening alloys with smaller projected crack length ratio λ and smaller cracking angle θ_c (as is also seen from Fig. 3(*b*)). In addition, the smaller value of λ gives larger displacements to separation in the higher hardening alloys than that of the lower hardening ones. An extension of this model by including another slip plane would admit a Mode I opening component (displacement not along the slip direction) and represent the general mixed mode case.

In the symmetric case, the crack penetration ratio (thinning of the ligament) P/l_0 was measured from the fracture surface profile plots and the cracking ratio q was found from (17). The values of P/l_0 for the alloys tested are shown in Table 1. The axial gauge displacement ratio u_a/l_0 was used in (14) to obtain the slip angle α. Then, equations (18) and (19) gave the values for the displacement ratio u_a/l_0, the penetration semiangle δ and the back angle β. Results for the HY-80 and A36 hot rolled steels are also shown in Table 2 and are compared with the experimental findings. Notice that the displacement for the symmetric case is more than twice that of the asym-

Table 1

Asymmetric	Projected length ratio, λ
1018 CF steel	0.890
HY-100 steel	0.820
HY-80 steel	0.850
A36 HR steel	0.770
1018 normalized steel	0.750
Symmetric	**Penetration ratio, P/l_0**
1018 CF steel	0.820
HY-100 steel	0.780
HY-80 steel	0.800
A36 HR steel	0.780
1018 Normalized steel	0.740

Table 2 Deformation of singly-grooved fully plastic specimens

Alloy:	HY-80 steel (low hardening)		A36 hot rolled (high hardening)	
Asymmetric. Assumed $\theta_s = 45$ deg				
Projected length ratio, λ, from tests	0.850		0.770	
Upper flank (cracking) angle, θ_c, from tests	39 deg		36 deg	
From	theory	tests	theory	tests
Growth Displ. ratio, u_a/l_0, equation (3)	0.150	0.115	0.230	0.216
Lower flank angle, θ_l, equation (6)	40.0 deg	41 deg	38.3 deg	41 deg
Back angle, β, equation (9)	7.4 deg	13 deg	10.6 deg	13 deg
Symmetric				
Penetration ratio, P/l_0, from tests	0.800		0.780	
Growth Displ. ratio, u_a/l_0, from tests	0.362		0.254	
From	theory	tests	theory	tests
Cracking ratio, q, from equation (17)	0.600		0.560	
Slip angle, α, equation (14)	42 deg		30 deg	
Penetration semiangle, δ, equation (18)	12.7 deg	13 deg	9.2 deg	10 deg
Back angle, β, equation (19)	10.5 deg	12 deg	17.3 deg	15.0 deg

metric case in the lower hardening HY-80 steel but not appreciably different between the two geometries in the higher hardening A36 hot rolled steel.

Conclusions

A macro-mechanical analysis for fully plastic Mode II crack growth along 45 deg slip bands, as might be encountered from cracks near a weld or shoulder, as well as for Mode I with two symmetric slip bands fully plastic crack growth, was developed. The model provides a physical basis for explaining the experimental findings on several alloys in both geometries. In the asymmetric shear specimens the crack is assumed to advance by sliding off along a single plane and fracture and the parameters of the macroscopic fracture (flank angles, crack opening angle, displacement to separation) can be found in terms of the projected flank length ratio and the cracking angle. In the symmetric case crack advance is assumed to occur by alternating shear along two symmetric slip planes followed by cracking and the fracture parameters are found in terms of the ratio of cracking to total reduction of ligament thickness.

Acknowledgments

The financial support of the Office of Naval Research, Arlington, Virginia, Contract N0014-82K-0025 is gratefully acknowledged. The author is also grateful to Professor Frank McClintock for valuable discussions.

References

1 Kardomateas, G., "Mixed Mode I and II Fully Plastic Crack Growth From Simulated Weld Defects," Ph.D. thesis, Department of Mechanical Engineering, M.I.T., 1985.

2 Shih, C. F., "Small Scale Yielding Analysis of Mixed Mode Plane-Strain Crack Problems," *Fracture Analysis*, ASTM STP 560, Am. Soc. Test. Mat., Philadelphia, 1974, pp. 187–210.

3 McClintock, F. A., and Slocum, A. H., "Predicting Fully Plastic Mode II Crack Growth from an Asymmetric Defect," *Int. J. Fract. Mechanics*, Vol. 27, 1985, pp. 49–62.

4 McClintock, F. A., "Plasticity Aspects of Fracture," *Fracture*, Vol. 3, edited by H. Liebowitz, Academic Press, New York, 1971, pp. 47–225.